iScience

CellPress
OPEN ACCESS

Article

A comparative study on the thermal runaway inhibition of 18650 lithium-ion batteries by different fire extinguishing agents

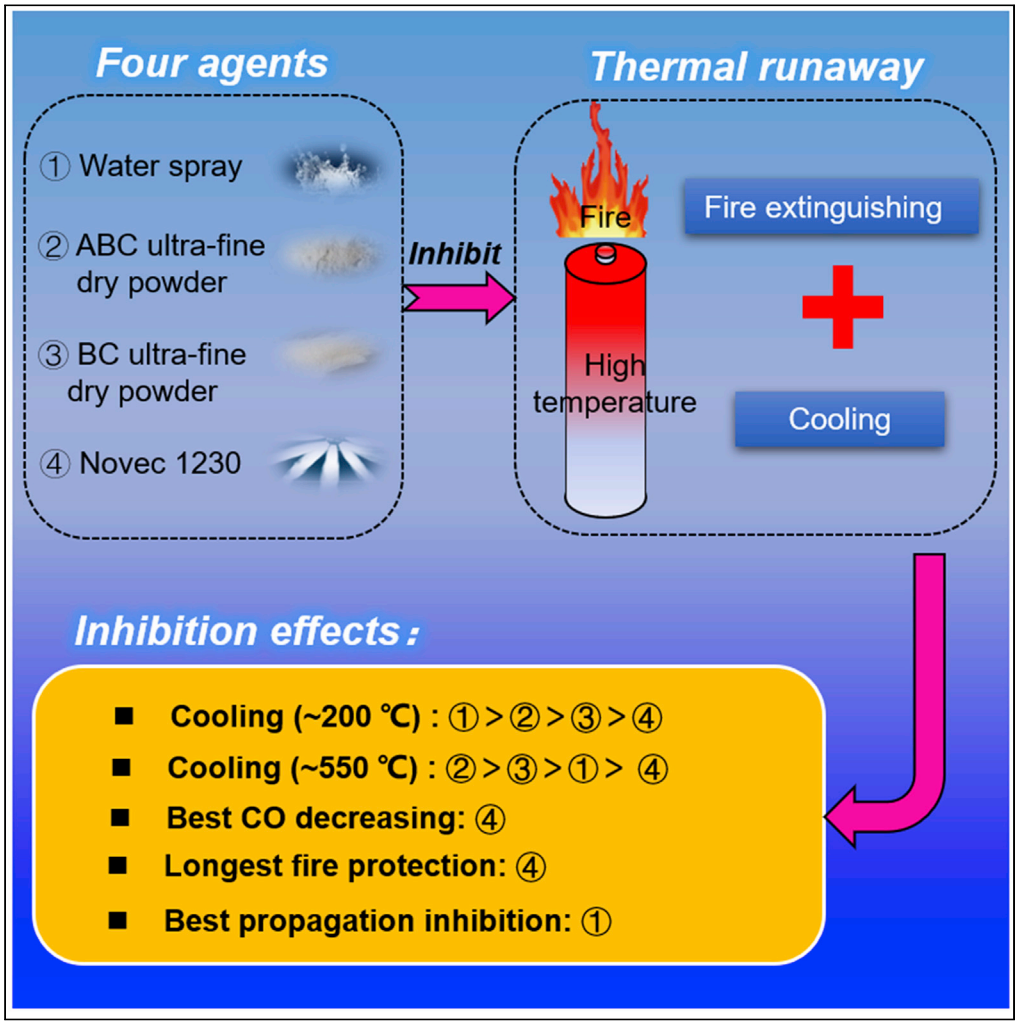

Junchao Zhao, Feng Xue, Yangyang Fu, Yuan Cheng, Hui Yang, Song Lu

yyfu@ustc.edu.cn (Y.F.)
lusong@ustc.edu.cn (S.L.)

Highlights

A comparative study was done on the inhibition effects of four suppressants

LIBs at 70% SOC had the best thermal runaway propagation ability

Water had the best cooling efficiency on LIBs being about to undergo TR

Novec 1230 existed in the enclosed space stably and protected LIBs from forming fires

Zhao et al., iScience 24, 102854
August 20, 2021
https://doi.org/10.1016/j.isci.2021.102854

iScience

CellPress
OPEN ACCESS

Article

A comparative study on the thermal runaway inhibition of 18650 lithium-ion batteries by different fire extinguishing agents

Junchao Zhao,[1] Feng Xue,[1] Yangyang Fu,[1,2,*] Yuan Cheng,[1] Hui Yang,[1] and Song Lu[1,*]

SUMMARY

Safety issue of lithium-ion batteries (LIBs) is always a concern. We have studied the inhabitation on thermal runaway (TR) and propagation of 18,650 LIBs in an enclosed space systematically. LIBs at 70% state of charge are chosen for testing. Four fire extinguishing agents are applied on LIB arrays for 20 s, and the inhibiting effects are different. The cooling efficiency varies with the surface temperatures of LIBs. Water spray has the highest cooling efficiency and inhibits the TR propagation among LIB arrays successfully. Three LIBs undergo TR for the releasing of ABC ultrafine dry powder. BC ultrafine dry powder and Novec 1230 are failed to inhibit the TR propagation. Nevertheless, Novec 1230 shows the best on inhibiting fire occurring and the generation of toxic gas. Generally, this study provides valuable information for the choice of fire extinguishing agents.

INTRODUCTION

Nowadays, with the demand of high energy density, long calendar, and high reliability for energy storage, lithium-ion batteries (LIBs) are widely used (Faessler et al., 2019; Wang et al., 2017). However, the safety issue is always a concern and accidents caused by LIBs cannot be completely avoided due to the instability of LIBs under abuse conditions (Liu et al., 2020a; Xu et al., 2021). The abuse conditions (i.e., thermal abuse [Wang et al., 2019b; Weng et al., 2019], electrical abuse [Feng et al., 2018b; Ren et al., 2019], and mechanical abuse [Yiding et al., 2020; Zhu et al., 2016, 2018]) will trigger thermal runaway (TR) of LIBs. While facing TR, complicated and violent chemical reactions inside LIBs occur proceeding with a significant amount of flammable and toxic gas and smoke (Wang and Wang, 2020). If there is no external interventions applying, TR continues and propagation between LIBs occurs, accompanied by fires or explosions (Chen et al., 2019).

To inhibit TR propagation, studies have done much (Said et al., 2020; Zhong et al., 2018). Heat transfer is considered to be the main cause of triggering TR in adjacent LIBs. Once a single LIB triggers TR, it is not hoped to cause transmission between LIBs. Hence, many attempts are done though designing separation layers (Larsson et al., 2016; Qin et al., 2019) and filling with heat-absorbing materials (Li et al., 2019a; Mohammed et al., 2019). However, if the protection does not work, passive protection is active aiming to reduce the TR damage (Larsson et al., 2014; Liu et al., 2020b; Wang et al., 2018).

Passive protection is the last barrier to prevent TR accidents expanding, and the effects are determined by fire extinguishing agents (Gao et al., 2019; Liu et al., 2019). Thus, the choice of fire extinguishing agents has become the focus of researchers and various tests have been carried out. The Federal Aviation Administration (Maloney, 2014) conducted the experiments on 18,650 LIBs fires under open spaces, pointing out that the aqueous agents were better than the nonaqueous agents in cooling effects and could prevent the TR propagation of the LIBs. Wang et al. (Wang et al., 2015) investigated the suppression efficiency of heptafluoropropane and dodecafluoro-2-methylpentan-3-one ($C_6F_{12}O$) on lithium titanate battery fires in an enclosed space. They found that heptafluoropropane and $C_6F_{12}O$ could extinguish the battery fire rapidly but could not inhibit the reignition of LIB fires (Wang et al., 2018). Liu et al. (Liu et al., 2019) verified that water mist could inhibit TR only if it was released before a critical temperature in a semiopen space. Meng et al. (Meng et al., 2020) found that dry powder could only extinguish LIB fires under the given specific conditions.

Though above analysis, numerous studies had been conducted to verify the effectiveness of various fire extinguishing agents on inhibiting TR of different LIBs TR. The research studies did give some references on the

[1]State Key Laboratory of Fire Science, University of Science of Technology of China, Hefei, Anhui, 230026, P.R.China

[2]Lead contact

*Correspondence: yyfu@ustc.edu.cn (Y.F.), lusong@ustc.edu.cn (S.L.)

https://doi.org/10.1016/j.isci.2021.102854

protection and fighting of LIB fires, though there were still some issues worthy of further discussion. For example, most experiments were conducted in open or semiopen spaces and the durability of fire suppression was ignored. The fire suppressing effects of different fire extinguishing agents at the same timescale could be meaningful. Also, there was a lack of quantitative comparison of fire extinguishing agents under the same experimental conditions. In addition, most experiments showed that the naked flame of LIBs was easier to extinguish (Wang et al., 2015). However, due to internal reactions continuing, the LIB fire was very easy to be reignited. Cooling was a way to weaken the internal reactions and reduce the fire risk (Liu et al., 2019). Therefore, it was necessary to consider both the timeliness and the cooling effects of the fire extinguishing agents.

Here, we compared the effects on the inhibition of TR fire and LIB TR propagation of four fire extinguishing agents (i.e., water spray, ABC and BC ultrafine dry powders, Novec 1230), which were chosen form three types of fire extinguishing agents: liquid, gas, and solid. TR experiments of single-LIB and LIB arrays were preconducted to determine the TR behaviors and exact parameters (i.e., trigger ability at different state of charges (SOCs), TR temperature, propagation time). Water was the most commonly used fire extinguishing agent, which was thought to have a high cooling efficiency. ABC ultrafine dry powder and BC ultrafine dry powder were often used for total submergence fire extinguishing in confined space as solids, verifying to have better fire extinguishing efficiency than water and gas fire extinguishing agents (Zhao et al., 2019, 2020a). Since the inhibition of battery TR should both consider cooling and fire extinguishing, gaseous fire extinguishing agent with high boiling point was first considered due to the latent heat of vaporization. Novec 1230 was a new, environmentally friendly, and efficient fire extinguishing agent with a high boiling point of 49.2°C and was used in various places replacing halons (Payri et al., 2020; Tang et al., 2020).

RESULTS

The TR behaviors of the single LIB

Before fire extinguishing experiments, the TR behaviors of the single LIB were firstly tested. As shown in Figure 1, under continuous heating, the LIB firstly underwent two stages of electrolyte leakage and safety valve opening (Henriksen et al., 2019). As the temperature rose, the electrolytes inside LIB evaporated and the inner pressure of LIB increased. Some electrolytes leaked from the safety valve. Once the inner pressure reached the design pressure of safety valve, it eventually led to the safety valve opening with massive smoke releasing. As the process continued, reactions became more dramatic proceeding with more smoke releasing. For the single LIB at 30% SOC, white smoke was emitted instantly as the LIB underwent complete TR. After that, the amount of releasing smoke decreased and eventually disappeared.

Compared with LIB at 30% SOC, LIB at 70% SOC emitted larger amount of smoke under TR. The LIB surface was heated to red, indicating a higher internal temperature. Molten aluminum spilt out from the safety valve and adhered to the LIB surface. The releasing gas was ignited and a naked flame appeared near the safety valve. Previous studies showed that the ignition temperature of flammable gases was between 500°C and 700°C (Addai et al., 2016; Chen et al., 2020; Lu et al., 2013). After 28 s of burning, the flame disappeared.

The more electricity stored, the more energy released during TR of LIB. While forming complete TR, hot particles injected. Aluminum foils melted at over 660°C and sprayed out from the LIB under high pressure. After that, a jet flame formed and it eventually transformed into a stable burning flame. When the storage energy of battery was released, the flame disappeared.

Figure 2A showed the surface temperature changes of LIBs at different SOCs under heating. When heated to about 500 s, all the curves decreased due to the safety valve open. The vaporized electrolytes were ejected instantly and took away massive heat from the LIBs, causing the temperature to decrease. However, the internal heat generation reaction was still going on, the temperature quickly rose again. Then, the curves rose rapidly and formed peaks. As shown in Figure 2B, as SOC increased, the safety valve open temperature decreased. For instance, the safety valve open temperature of LIBs at 0% and 100% SOCs were 200.5°C and 183.1°C, respectively. The TR peak temperatures increased with the increasing SOCs. It was proved that the heat released from the LIBs during TR was almost equal to the electrical energy (Feng et al., 2018a). The peak temperature of the LIB at 100% SOC was 703.6°C, which was more than twice that of the LIB at 0% SOC.

Mass loss was also an important parameter of TR behaviors of LIBs. The higher SOC, the more mass loss. At 0% SOC, the mass loss was 3.9 g. The mass loss of LIBs at 70% SOC was 6.7 g, which was 0.3 g more than that of LIBs at 50% SOC. However, the mass loss of LIBs at 100% SOC was 15.6 g, 2.3 times higher than that of

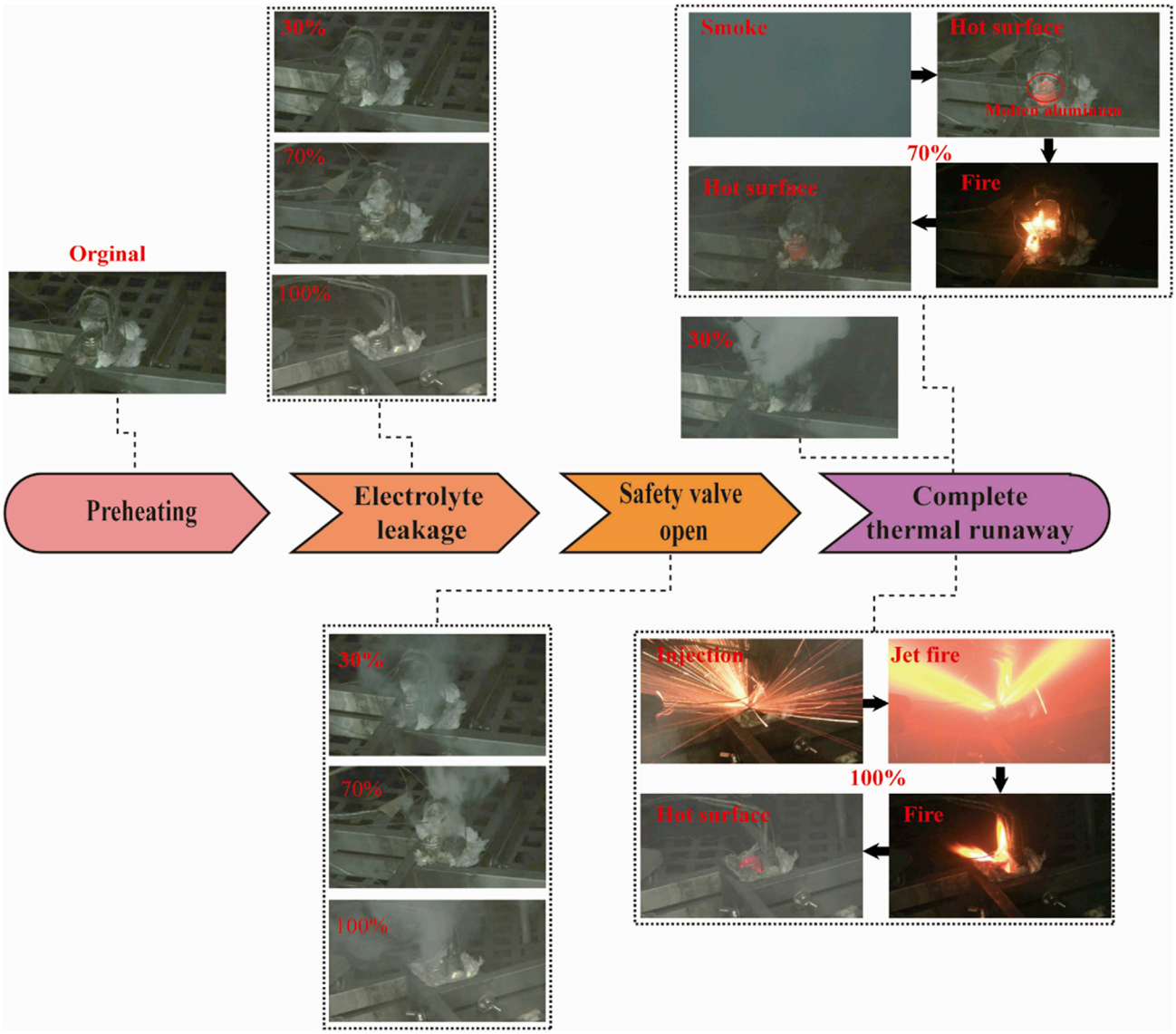

Figure 1. The TR behaviors of single-LIB at different SOCs

LIBs at 70% SOC. The more dramatic TR process indicated more energy released. Especially, the injecting of molten aluminum particles caused the most mass loss.

The TR behaviors of LIB arrays

As shown in Figure S1, the propagation characters for LIB arrays at different SOCs were different. Under heating, NO.1 LIB went into TR proceeding with the same TR phenomenon described in chapter 3.1. When NO.1 LIB was triggered to complete TR and reached the peak temperature, the surface temperature of NO.2 LIB was 60–150°C, varying with the SOCs. Then, due to the exist of temperature difference between NO.1 and NO.2 LIBs, the temperature of NO.2 increased rapidly. According to Arrhenius's law, if only the heat input to the system was greater than the heat dissipated, it would eventually lead to thermal runaway of the system (Huang et al., 2019). The heat input to NO.2 LIB contained the heat transfer (q_{con}) from NO.1 LIB to NO.2 LIB and the self-reacting heat (q_{gen}) of NO.2 LIB, as shown in Figure 3. At the same time, the heat dissipation of NO.2 LIB was due to the heat conduction (q'_{con}) from NO.2 to NO.3, and natural convection (q_{air}) with the air. Basing on the finished results, the 18,650 LIB would self-heat when it reached 89–130°C (T_{onset}) (Mao et al., 2020). It means, only when $T_{NO.2}>T_{onset}$, the value of q_{gen}

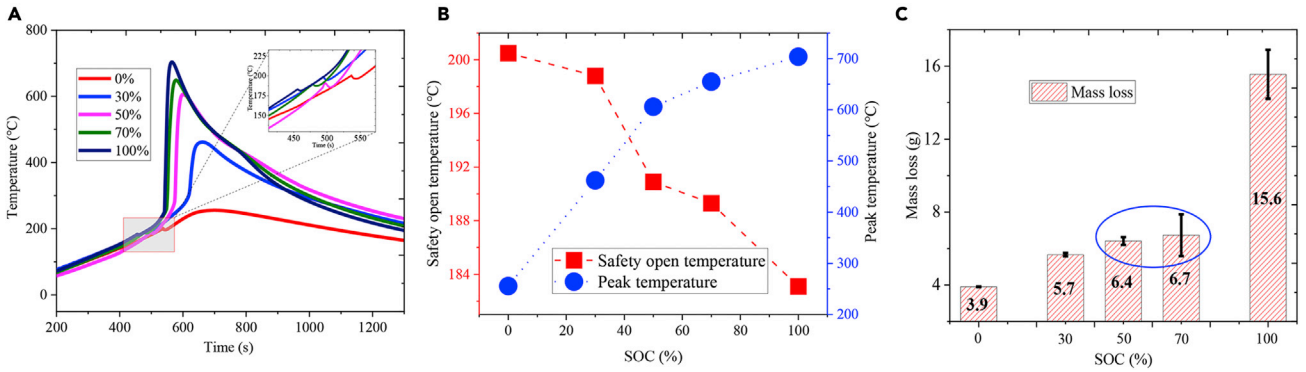

Figure 2. TR test of single LIB

(A) The curves of surface temperature evolution for the heated LIBs at different SOCs.

(B) The safety-open temperature and peak temperature for the curves of temperature evolution.

(C) Mass loss of LIBs at different SOCs.

was greater than 0. For the TR propagation, if (q_{con}- q'_{con}) was equal to q_{air}, $T_{NO.2}$ was still less than T_{onset}, and the system would not be triggered TR. Since NO.2 LIB was in a nonadiabatic state, $T_{NO.2}$ needed to be much larger than T_{onset} to cause TR. It was found that NO.1 LIBs at 30% and 100% SOCs did not trigger TR of other LIBs. The third LIB of LIB arrays at 50% SOC underwent TR. LIB arrays at 70% SOC had the strongest propagation capability and all the LIBs went into TR.

In Figure 4A, the peak temperatures of different LIB arrays were given. The maximum temperature of LIB arrays at 30% SOC was 450.6°C, and it did not cause TR of other LIBs. Though NO.1 LIB at 100% SOC reached 794.0°C, the other LIBs were not triggered TR, either. LIB arrays at 70% SOC all underwent TR, and the average temperature was 713.0°C. The differences in propagation ability could be explained from Equation 1.

$$Q_{s,max} = C_b M_b (T_{max} - T_E) \quad \text{(Equation 1)}$$

$Q_{s,\ max}$ represents the maximum storage heat inside an LIB; C_b represents the specific heat capacity of LIB, 850 J/(kg·K) (Huang et al., 2021); M_b represents the mass of LIB; T_{max} represents the TR maximum temperature; T_E represents the environmental temperature, 288.15 K. The LIBs of different SOCs maximum storage heat was calculated, which was shown in Table 1. Though NO.1 LIB at 100% SOC had the highest T_{max}, the storage heat was 16.60 kJ, which was less than that of the LIBs at 50% and 70% SOCs. The TR peak temperatures of LIBs at 50% SOC varied a lot. When NO.3 LIB was triggered complete TR, NO.4 LIB was heated to 140°C and not triggered TR eventually. From another perspective, since the different propagation of NO.1 LIBs at 50% and 100% SOCs, the value of critical storage heat to trigger TR should be between 16.60 and 19.26 kJ. While facing TR, the maximum storage heat of NO.3 LIB at 50% was only 13.31 kJ.

As shown in Figure 4B, the propagation times of LIB arrays at 50% and 70% SOCs were given. The data was calculated based on the time when LIBs reached the peak temperatures. For LIB arrays at 70% SOC, the TR propagation time was 74 s, 146 s and 129 s. Only three LIBs at 50% SOC went into TR, and the time intervals were 132 s and 130 s, respectively. Generally, the average propagation time of LIB arrays at 70% SOC was 116 s, which was less than that of LIBs at 50% SOC (i.e., 131 s). Thus, 70% SOC were chosen as experimental charge due to the strongest propagation ability.

Suppressing on TR fire and TR propagation of LIB arrays

The main reason for the TR propagation was that the LIB suffered from TR heats including flame radiation and the shell heat transfer. As shown above, when a single LIB suffered from TR, the surface temperature reached a high level, proceeding with the phenomenon of fire and gas production. The key to inhibit TR propagation was to quickly reduce the surface temperature of LIB to a safe range. To ensure the fire extinguishing agents were not spraying out with in specified time, the spraying duration was set as 20 s. When the first LIB underwent safety open, the heater was turned off. The first LIB would undergo TR and then trigger the second LIB. Once safety valve of the second LIB opened, the solenoid valve opened. The fire

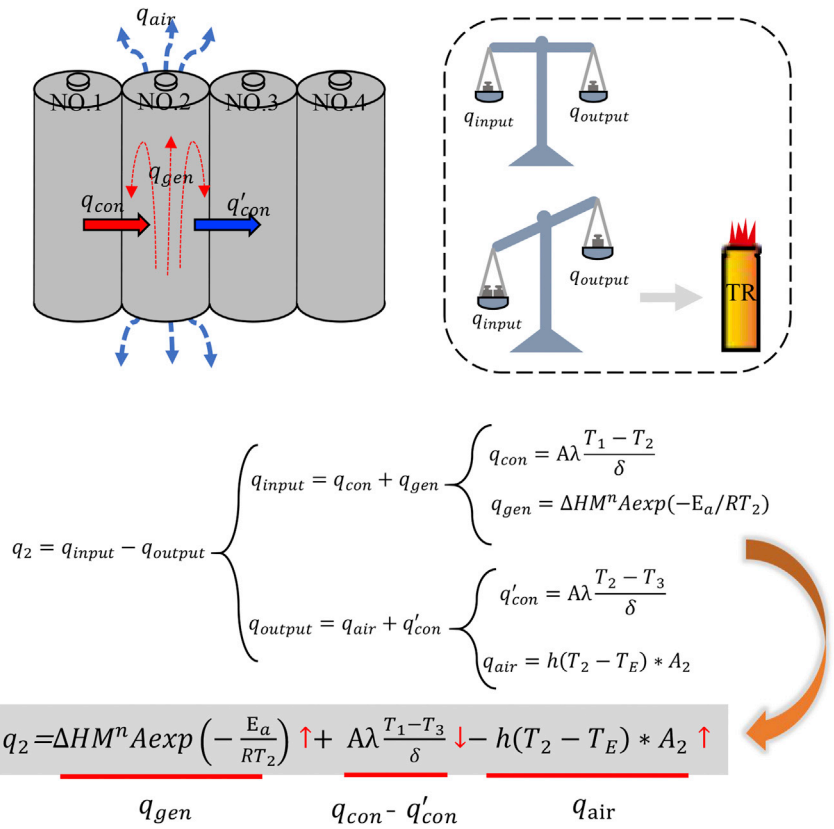

Figure 3. The process of NO.2 LIB being triggered TR

q_{input}, heat input rate; q_{output}, represents heat output rate; $q_{NO.2}$, total heat rate of NO.2 battery; q_{con}, heat conduction input heat rate; q_{gen}, reaction exotherm rate; q_{air}, natural convection heat dissipation rate; q'_{con}, heat conduction output rate; A, heat conduction area; $A_{NO.2}$, natural convection heat dissipation area of NO.2 battery; λ, thermal conductivity; $T_{NO.1}$, average temperature of NO.1 battery; M_b, LIB mass; $T_{NO.2}$, average temperature of NO.2 battery; $T_{NO.3}$, average temperature of NO.3 battery; T_E, average temperature of environment; δ, thickness of heat-conducting object; ΔH, reaction calorific value of per mass; M, mass; n, reaction order; h, convection heat transfer coefficient.

extinguishing agents would be driven by nitrogen gas and sprayed through the nozzle. In Figure 5, the surface temperature curves of LIB arrays under different conditions were given.

Without applying any agents, all four LIBs formed TR. When the safety valve of NO.2 LIB opened, the valve 2 was turned on and the fire extinguishing agents were kept spraying for 20 s. During the releasing of the fire extinguishing agents, the LIB surface temperature formed varying degrees of decline. While water was applying, the upper and lower surface temperature of NO.1 LIB dropped by 324.5°C and 54.6°C, respectively. For NO.2 LIB, the temperature drop gradients on the upper and lower surfaces were 110°C and 47.6°C, respectively. Water had the best cooling efficiency and TR process was efficiently suppressed. After injecting ABC ultrafine dry powder, NO.2 LIB still eventually went into complete TR. However, it did not propagate to NO.3 LIB, as shown in Figure 5C. The temperature dropping gradients on the upper and lower surfaces of NO.1 LIB were 271.3°C and 201.6°C, respectively. For NO.2 LIB, they were 84.2°C and 36.0°C. BC ultra-fine dry powder and Novec 1230 were failed to suppress the propagation of LIB arrays. The injection of BC ultrafine dry powder caused the upper and lower surface temperatures of NO.1 and NO.2 LIBs dropping by 255.7°C and 37.5°C, 92.6°C and 13.6°C, respectively.

However, instant temperature decline might not fully reflect the cooling efficiency of fire extinguishing agents and the temperature would rerise. Research had shown that the instant temperature drop might reflect the temperature of agents (Huang et al., 2021). It was assumed that during the applying of agents, the air convection heat and the radiation heat of LIBs were ignored. The temperature reduction ($\Delta T_{a-r,\,i}$) caused by the agent could be calculated by Equation 2. Thus, the cooling efficiency could be reflected

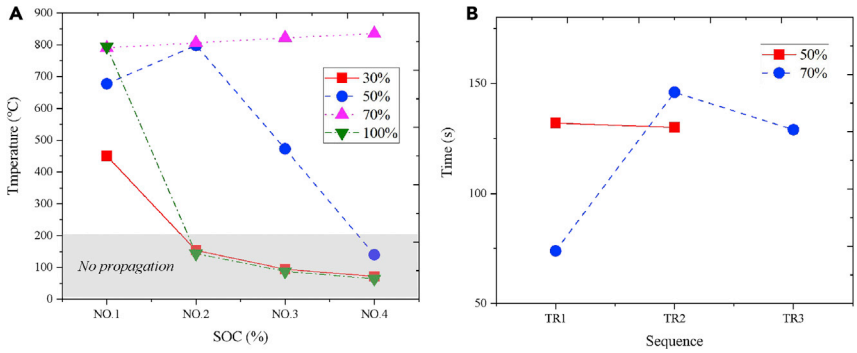

Figure 4. The comparison of propagation capability of LIB arrays at different SOCs

(A) Peak temperature of LIB arrays.

(B) The TR propagation time of LIBs arrays at 50% and 70% SOCs.

by the heat absorbing ($Q_{ab,i}$) form LIBs of agents, which was calculated by Equation 3. $T_{a,i}$ represented the temperature as agents applying and $T_{a,i}$ represented the re-increase temperature after agents applying.

$$\Delta T_{a-r,\,i} = T_{a,\,i} - T_{r,\,i} \quad \text{(Equation 2)}$$

$$Q_{ab,\,i} = C_b M_b \Delta T_{a-r,\,i} \quad \text{(Equation 3)}$$

As shown in Table 2, the cooling efficiency of agents on NO.1 and NO.2 LIBs varied a lot. For NO.1 LIB, the rank of cooling efficiency was ABC dry powder > BC dry powder > water spray > Novec 1230. However, water spray had the best cooling efficiency on NO.2 LIB. The same results were also found from the absorption heat. The main reason was due to the different temperatures of NO.1 and NO.2 LIBs when agents were released. The water droplets contacted with LIB surfaces and then evaporated. With the bolt temperature of 100°C, larger temperature difference should lead to a higher heat conversion efficiency. The powder agents were different with the way of water cooling. After applying, part of powder agents settled and covered the surfaces. Therefore, the cooling time of powders would be longer than water, especially at higher temperature. The initial decomposition temperatures of ABC and BC ultrafine dry powders were 193.5°C and 106.0°C, respectively (shown in Figure S2). The temperature of NO.2 LIB at the time of agents releasing was about 200°C. So, the cooling efficiencies were always worse than water. In addition, the latent heat of ABC ultrafine dry powder was 1050.3 J/g, larger than that of BC ultrafine dry powder, 660.52 J/g. Thus, for LIBs with high temperature, ABC ultrafine dry powder had a batter cooling efficiency, Nover 1230 was had the worst efficiency during the test. Maybe, a suitable injection way should be found.

In Table 3, after 20 s releasing, water consumed 559.5 g, which was the most. Though the filling weight of Novec 1230 was larger than that of water, it consumed less. This was attributed to the lager viscosity of Novec 1230 causing it hard to be injected. The consumption of ABC ultrafine dry powder was 343.1 g, which was 1.5 times that of BC ultrafine dry powder.

As shown in Figure 6A, LIB arrays under BC ultrafine dry powder and Novec 1230 suppressing showed few differences with LIB arrays with no fire extinguishing agents. The average maximum temperatures of LIB arrays under no agents, BC ultrafine dry powder, and Novec 1230 were 760.4°C, 778.1°C, and 783.9°C, respectively. The data of LIB arrays under water spray repeated better. Only NO.1 LIB heated by the heater went into TR and NO.2 LIB was heated to a maximum temperature of 226.3°C. ABC ultrafine dry powder had effects on inhibiting TR propagation of LIB arrays, but it was weaker than water spray. Only NO.4 LIB had never gone into TR. In Figure 6B, though BC powder and Novec 1230 were applied to suppress, they had few influences on the propagation time. The average propagation times of no agents, BC powder, and Novec 1230 were 186 s, 192 s, and 186 s, respectively.

As shown in Figure 7, CO concentrations under different conditions were measured to verify the ability of suppressants on inhibiting toxic gas generation. Without any agents, the curve formed four stages corresponding to TR processes of four LIBs and the CO concentration was the largest. When agents were released, CO concentrations decreased. The curves of BC powder and Novec 1230 both had four stages, similar with the curve of no agents. However, the maximum CO concentration with BC powder and Novec 1230 applying were 3897 ppm

Table 1. The LIBs of different SOCs maximum storage heat under testing

	Average $Q_{s,\ max}$ (kJ)			
SOCs (%)	NO.1	NO.2	NO.3	NO.4
30	12.94	4.78	2.74	1.98
50	19.26	22.77	13.31	4.31
70	22.33	22.79	23.23	23.62
100	16.60	4.43	2.52	1.71

and 1952 ppm, which verified that the two agents could inhibit the generation of CO. Especially, Novec 1230 had the better efficiency. Novec 1230 had chain chemical reactions with the LIB electrolyte (Wang et al., 2019a), so its effect on decreasing the CO content was much better than other agents. Water spray and ABC powder inhibited TR propagation, and thus, it was hard to compare their efficiency on CO generation.

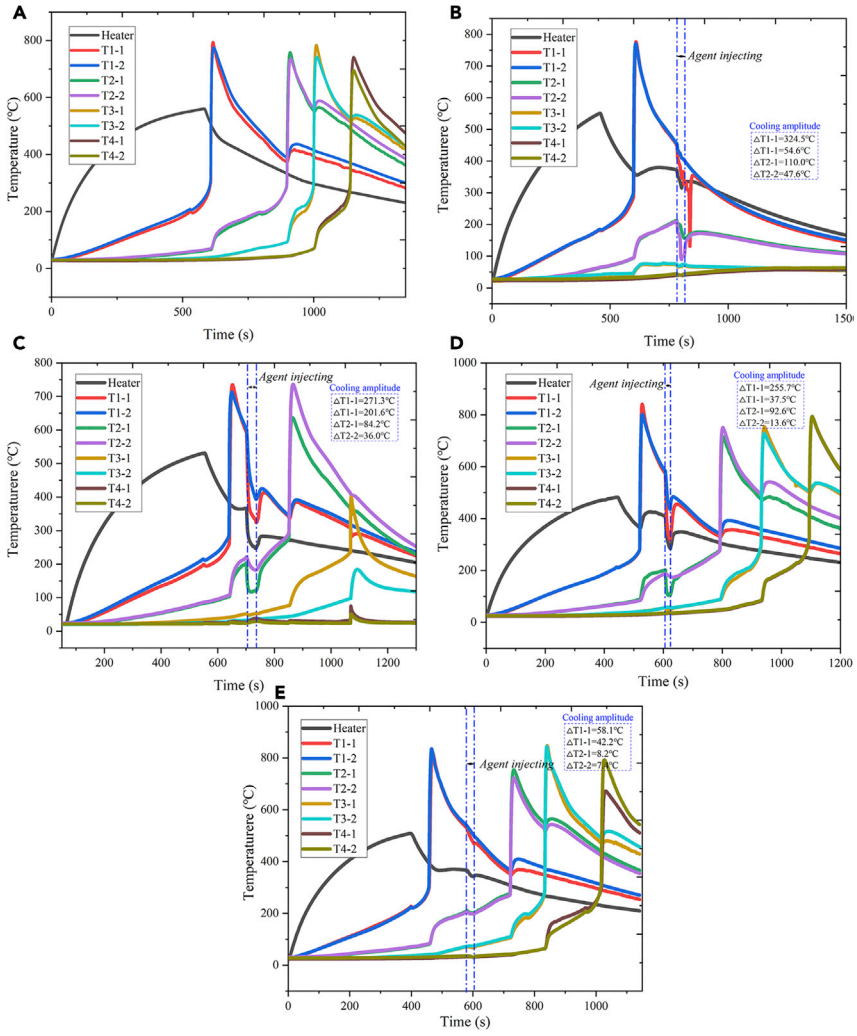

Figure 5. LIB surface temperature curves with different fire extinguishing agents

(A) no agents.

(B) water spray.

(C) ABC ultrafine dry powder injecting.

(D) BC ultrafine dry powder injecting.

(E) Novec 1230 injecting.

Table 2. The reduction temperature and absorbed heat of different LIBs

Agents	$\Delta T_{a-r,\ NO.1}$ (°C)	$\Delta T_{a-r,\ NO.2}$ (°C)	$Q_{ab,\ NO.1}$ (kJ)	$Q_{ab,\ NO.2}$(kJ)
Water spray	90.05	40.68	2.59	1.40
ABC dry powder	175.49	19.70	5.05	0.68
BC dry powder	110.15	4.40	3.17	0.15
Novec 1230	48.60	3.60	1.40	0.12

Discussion on the choice of fire extinguishing agents

As can be shown in Figure 8A, when NO.1 LIB went into complete TR, NO.2 LIB was heated to safety open quickly and then suppressants were injecting. Under heating, NO.1 LIB underwent safety valve open and flammable gas releasing. The flammable gas, also called LIB vent gas (BVG), was thought to be closely to the explosion or fire of LIBs (Fernandes et al., 2018; Kumai et al., 1999). The BVG is generated during the TR process (i.e., the decompositions of the negative solid–electrolyte interface film, reactions of anode with the electrolytes, decompositions of inner materials, and reactions between various material decomposition products) (Li et al., 2019b). BVG mainly included carbon monoxide (CO), hydrogen (H_2), and hydrocarbons such as methane (CH_4), ethylene (C_2H_4), and ethane (C_2H_6) (Somandepalli et al., 2014). Once the TR temperature reached the ignition temperature, BVG was ignited and a steady naked fire formed. Sometimes, if the mixing gas of BVG and air in the box reached the lower explosion limit, an explosion would occur (Zhang et al., 2019).

As a kind of good cooling material, water was used for fire suppressing for a long time (Ni and Chow, 2011). Thus, for water spray, cooling was the main suppression mechanism. Better cooling efficiency caused the propagation to be inhibited. When water was dispersed into droplets and contacted with the hot surface of LIBs, it quickly absorbed heat and reduced the LIB surface temperatures. However, due to the high boiling point at the standard state (100°C), the cooling effect was not so obvious at low temperatures.

Due to the smaller particle size, ABC and BC ultrafine dry powders had total flooding fire extinguishing ability (Zhao et al., 2020a, 2020b). That means, after injecting, the powders could fill the entire space and inhibit fires and explosions (Jiang et al., 2019; Yu et al., 2016). During actual experiments, it was also found that the covering layer of powders had the effects on reducing LIB surface temperature. Comparing only these two extinguishing agents, ABC ultrafine powder had a better cooling effect than BC ultrafine powder. ABC powder had good thermal efficiencies due to more mass loss and heat absorption. In Figure 8C, suppressing by ABC powder effectively inhibit TR propagation, as LIB arrays suppressed by BC powder all went into TR and the covering layer were burnt.

In Figure 8D, Novec 1230 had three mechanisms of suppressing the LIB TR. Actually, due to the low boiling point of 49.2°C, Novec 1230 evaporated quickly and absorbed much heat form environment causing environment temperature decrease, as shown in Figure 9. Little Novec 1230 contacted with LIB surfaces and the cooling effect was the worst among the four suppressants. In addition, the evaporated Novec 1230 reached certain concentration, it could inhibit fires and explosions. In Figure 9, the curves of no agents exhibited a peak caused by LIB fire. Under fire extinguishing agents applying, no peaks formed which verified the fire was inhibited. Due to the failure of TR inhibition of ABC ultrafine dry powder, BC ultrafine dry powder and Novec 1230, all the agents had the ability to provide long time protection forming fires. Nevertheless, vaporized Novec 1230 had even longest protection time.

Table 3. Agent consumptions and suppressing effects

		Consumption of agent quality (g)			The number of TR LIBs	
Agents	LIB type	Test 1	Test 2	Average	Test 1	Test 2
Water	SAMSUNG 18650	588.8	530.2	559.5	1	1
ABC ultrafine dry powder		337.9	348.2	343.1	2	3
BC ultrafine dry powder		243.3	213.4	228.4	4	4
Novec-1230		391.7	456.0	423.9	4	4

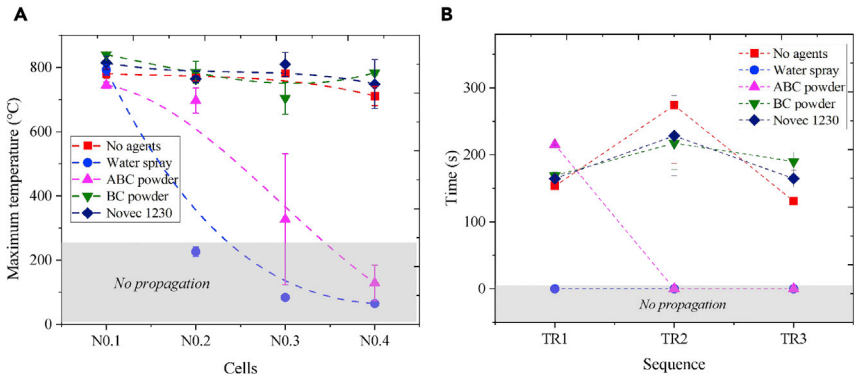

Figure 6. The comparison of propagation capability of LIB arrays with different fire extinguishing agents

(A) Maximum temperature of LIB arrays under suppressing.

(B) Propagation time of LIB arrays TR under suppressing.

As illustrated in Figure 8E, fire and high temperature were the main LIB TR behaviors. High temperature was thought to be the main cause to trigger TR of other LIBs. Fire could expand the hazard to other LIBs and combustible objects across space. Therefore, one aspect of TR inhibition strategy was to cool the LIB to prevent the propagation. Another aspect is to ensure that there is no fire in the confined space. Among the four fire extinguishing agents, water spray had the best cooling efficiency, but it consumed the most weight. Once the TR was not suppressed under a certain amount of water, it had few effects on the subsequent TR process. Moreover, the extensive use of water could cause short circuit of LIB modules and cause greater disasters. ABC ultrafine dry powder, BC ultrafine dry powder, and Novec 1230 all had the total flooding fire extinguishing abilities. However, powder would settle and eventually loss fire prevention capacities. It was found the covering layer of powders could cool down the LIB surface temperature through thermal decomposition and heat absorption. Novec 1230 could decrease the ambient temperature, but the cooling effect on the specified TR LIB was not obvious. Since the mixed gas existed stably, it could prevent fire or explosion occurring once the use concentration was reached. If possible, the combined use of water and Novec 1230 could achieve a better result.

Conclusion

In conclusion, the research systematically studied four fire extinguishing agents (i.e., water spray, ABC and BC ultrafine dry powder, Novec 1230) on TR fires and TR propagation of the 18,650 LIBs. The important results could be concluded as follows:

(1) As SOC increased, the LIB safety valve open temperature decreased and the TR peak temperature increased. LIBs at 100% SOC injected molten aluminum particles, resulting in the largest mass loss, which was 2.3 times of LIBs at 70% SOC.

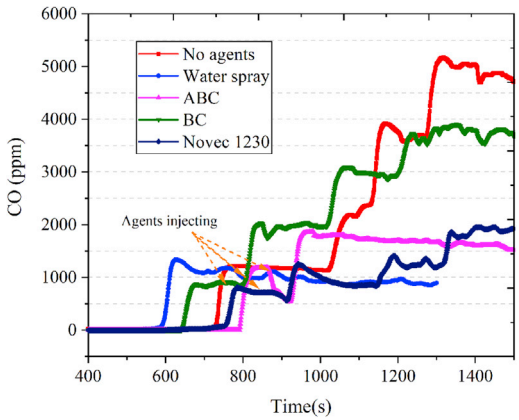

Figure 7. CO concentrations under different conditions

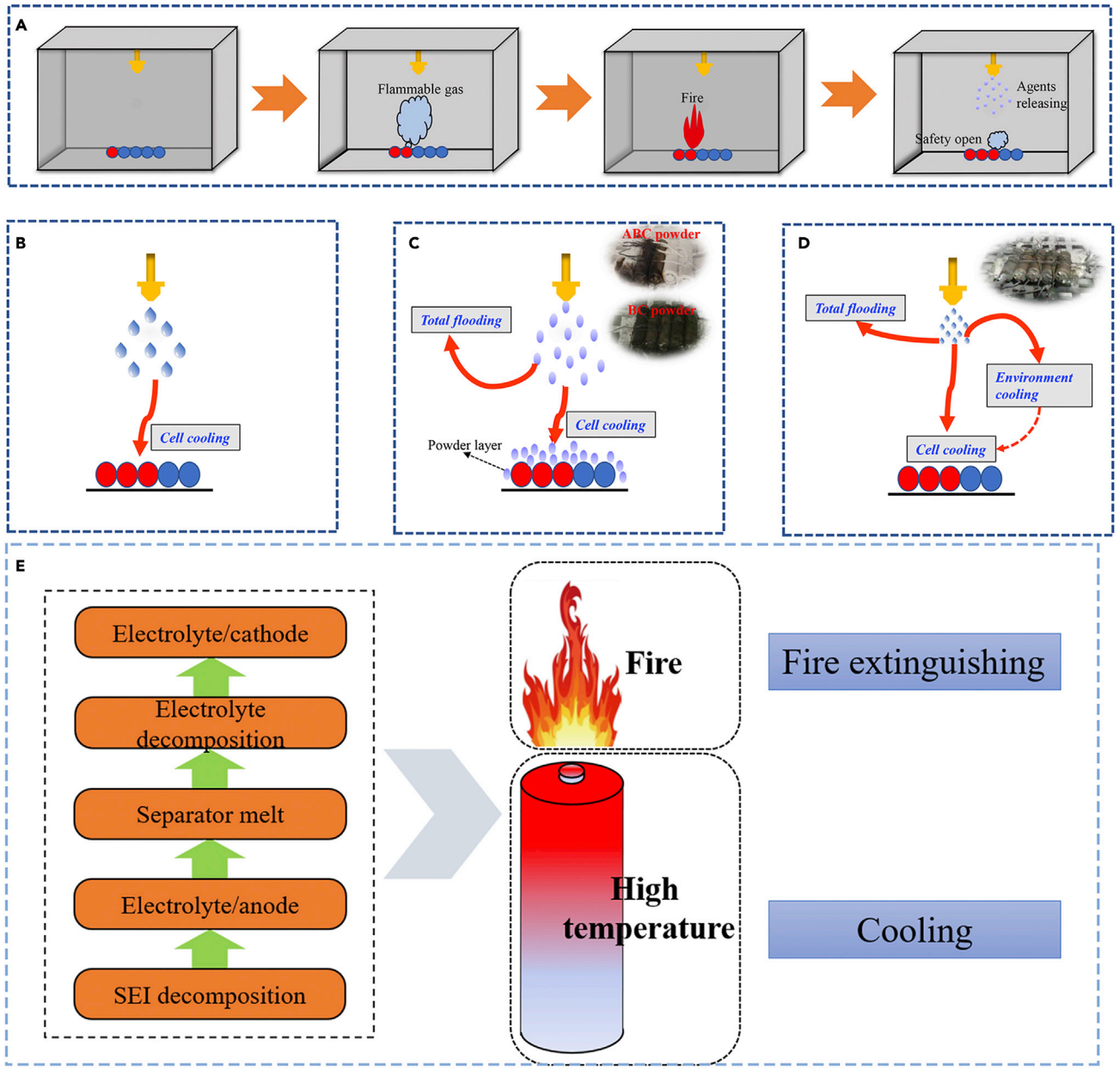

Figure 8. The detailed inhibition mechanism by different fire extinguishing agents

(a) TR propagation behaviors in the experimental box.

(b) Suppression mechanism of water spray.

(c) Suppression mechanism of ABC and BC ultrafine dry powder.

(d) Suppression mechanism of Novec 1230.

(e) Mechanism of TR prevention.

(2) LIBs at 70% SOC had the strongest TR propagation capacity. All four LIBs underwent TR of LIB arrays at 70% SOC, while two LIBs underwent TR of LIB arrays at 50% and only single LIB underwent TR of LIB arrays at 30% and 100%. Though NO.1 LIB at 100% SOC reached 794.0°C, the storage heat was 16.60 kJ, even less than LIBs at 50% SOC (19.26 kJ). It was found the value of critical storage heat to trigger TR should be between 16.60 and 19.26 kJ.

(3) For LIBs with different surface temperatures, the cooling efficiencies were different. As agents applying, NO.1 and NO.2 LIBs were about 550°C and 200°C, respectively. For NO.1 LIB, the fire

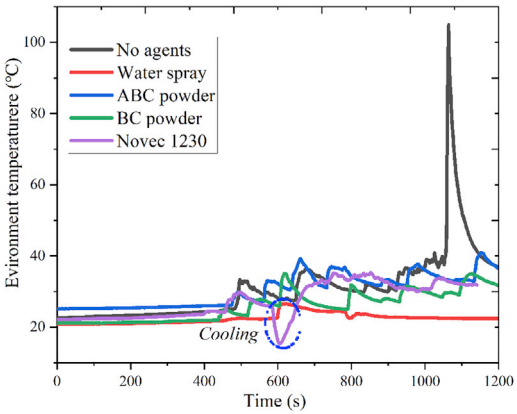

Figure 9. Environment temperature changes under different conditions

extinguishing agent cooling efficiency rank was ABC ultrafine dry powder > BC ultrafine dry powder > water spray > Novec 1230. However, for NO.2 LIB, water spray had the best cooling efficiency and inhibited TR propagation successfully. Comparison from the cooling effects on NO.2 LIB, water spray > ABC ultrafine dry powder > BC ultrafine dry powder > Novec 1230. The cooling effects of Novec 1230 were limited by releasing method. Spray caused most agents evaporating before contacting with LIB due to the small droplets and low evaporation temperature.

(4) Novec 1230 had the best effect on decreasing the CO content among the four agents. Also, Novec 1230 vapor could exist in the enclosed space for a long time and protect the LIB forming fires.

(5) The combined use of water and Novec 1230 may achieve a better result.

Limitations of the study

In this paper, we only gave the representative comparative results of four fire extinguishing agents. To get more practical suggestions, more fire extinguishing agents need to be tested and more actual application scenarios need to be considered.

STAR★METHODS

Detailed methods are provided in the online version of this paper and include the following:

- KEY RESOURCES TABLE
- RESOURCE AVAILABILITY
  - Lead contact
  - Materials availability
  - Data and code availability
- METHOD DETAILS
  - The pretreatment of 18650 batteries
  - The choice of fire extinguishing agents
  - The TR pretest layout of single LIB and LIB arrays
  - Experimental setup of fire extinguishing on the TR inhibition of LIB arrays

SUPPLEMENTAL INFORMATION

Supplemental information can be found online at https://doi.org/10.1016/j.isci.2021.102854.

ACKNOWLEDGMENTS

This work was supported by the National Natural Science Foundation of China (No. 51804288). Also, it was supported by the National Key R&D Program of China (No. 2018YFC0807605), the National Natural Science Foundation of China (No.51974284), the Fundamental Research Funds for the Central Universities under Grant No. WK2320000046.

AUTHOR CONTRIBUTIONS

Conceptualization, J.Z. and Y.F.; formal analysis, J.Z., Y.F., Y.C., and H.Y.; investigation, J.Z., F.X., and Y.F.; data curation, J.Z., F.X., and Y.C.; writing - original draft, J.Z.; resources, supervision and writing - review & editing, Y.F. and S.L.; project administration, S.L.; all authors discussed the results and contributed to the manuscript.

DECLARATION OF INTERESTS

The authors declare no competing interests.

Received: May 9, 2021
Revised: June 18, 2021
Accepted: July 9, 2021
Published: August 20, 2021

REFERENCES

Addai, E.K., Gabel, D., and Krause, U. (2016). Experimental investigation on the minimum ignition temperature of hybrid mixtures of dusts and gases or solvents. J. Hazard Mater. *301*, 314–326. https://doi.org/10.1016/j.jhazmat.2015.09.006.

Chen, M., Dongxu, O., Liu, J., and Wang, J. (2019). Investigation on thermal and fire propagation behaviors of multiple lithium-ion batteries within the package. Appl. Therm. Eng. *157*, 113750. https://doi.org/10.1016/j.applthermaleng.2019.113750.

Chen, S., Wang, Z., Wang, J., Tong, X., and Yan, W. (2020). Lower explosion limit of the vented gases from Li-ion batteries thermal runaway in high temperature condition. J. Loss Prev. Process Ind. *63*, 103992. https://doi.org/10.1016/j.jlp.2019.103992.

Faessler, B., Kepplinger, P., and Petrasch, J. (2019). Field testing of repurposed electric vehicle batteries for price-driven grid balancing. J. Energy Storage *21*, 40–47. https://doi.org/10.1016/j.est.2018.10.010.

Feng, X., Ouyang, M., Liu, X., Lu, L., Xia, Y., and He, X. (2018a). Thermal runaway mechanism of lithium ion battery for electric vehicles: a review. Energy Storage Mater. *10*, 246–267. https://doi.org/10.1016/j.ensm.2017.05.013.

Feng, X., Zheng, S., He, X., Wang, L., Wang, Y., Ren, D., and Ouyang, M. (2018b). Time sequence map for interpreting the thermal runaway mechanism of lithium-ion batteries with LiNixCoyMnzO2 cathode. Front. Energy Res. *6*, 00126. https://doi.org/10.3389/fenrg.2018.00126.

Fernandes, Y., Bry, A., and de Persis, S. (2018). Identification and quantification of gases emitted during abuse tests by overcharge of a commercial Li-ion battery. J. Power Sourc. *389*, 106–119. https://doi.org/10.1016/j.jpowsour.2018.03.034.

Gao, Q., Liu, Y., Wang, G., Deng, F., and Zhu, J. (2019). An experimental investigation of refrigerant emergency spray on cooling and oxygen suppression for overheating power battery. J. Power Sourc. *415*, 33–43. https://doi.org/10.1016/j.jpowsour.2019.01.052.

Henriksen, M., Vaagsaether, K., Lundberg, J., Forseth, S., and Bjerketvedt, D. (2019). Explosion characteristics for Li-ion battery electrolytes at elevated temperatures. J. Hazard Mater. *371*, 1–7. https://doi.org/10.1016/j.jhazmat.2019.02.108.

Huang, P., Chen, H., Verma, A., Wang, Q., Mukherjee, P., and Sun, J. (2019). Non-dimensional analysis of the criticality of Li-ion battery thermal runaway behavior. J. Hazard Mater. *369*, 268–278. https://doi.org/10.1016/j.jhazmat.2019.01.049.

Huang, Z., Liu, P., Duan, Q., Zhao, C., and Wang, Q. (2021). Experimental investigation on the cooling and suppression effects of liquid nitrogen on the thermal runaway of lithium ion battery. J. Power Sourc. *495*, 229795. https://doi.org/10.1016/j.jpowsour.2021.229795.

Jiang, H., Bi, M., Li, B., Ma, D., and Gao, W. (2019). Flame inhibition of aluminum dust explosion by NaHCO3 and NH4H2PO4. Combustion Flame *200*, 97–114. https://doi.org/10.1016/j.combustflame.2018.11.016.

Kumai, K., Miyashiro, H., Kobayashi, Y., Takei, K., and Ishikawa, R. (1999). Gas generation mechanism due to electrolyte decomposition in commercial lithium-ion cell. J. Power Sourc. *81-82*, 715–719. https://doi.org/10.1016/S0378-7753(98)00234-1.

Larsson, F., Anderson, J., Andersson, P., and Mellander, B.-E. (2016). Thermal modelling of cell-to-cell fire propagation and cascading thermal runaway failure effects for lithium-ion battery cells and modules using fire walls. J. Electrochem. Soc. *163*, A2854–A2865. https://doi.org/10.1149/2.0131614jes.

Larsson, F., Andersson, P., Blomqvist, P., Lorén, A., and Mellander, B.-E. (2014). Characteristics of lithium-ion batteries during fire tests. J. Power Sourc. *271*, 414–420. https://doi.org/10.1016/j.jpowsour.2014.08.027.

Li, Q., Yang, C., Santhanagopalan, S., Smith, K., Lamb, J., Steele, L.A., and Torres-Castro, L. (2019a). Numerical investigation of thermal runaway mitigation through a passive thermal management system. J. Power Sourc. *429*, 80–88. https://doi.org/10.1016/j.jpowsour.2019.04.091.

Li, W., Wang, H., Zhang, Y., and Ouyang, M. (2019b). Flammability characteristics of the battery vent gas: a case of NCA and LFP lithium-ion batteries during external heating abuse. J. Energy Storage *24*, 100775. https://doi.org/10.1016/j.est.2019.100775.

Liu, B., Jia, Y., Yuan, C., Wang, L., Gao, X., Yin, S., and Xu, J. (2020a). Safety issues and mechanisms of lithium-ion battery cell upon mechanical abusive loading: a review. Energy Storage Mater. *24*, 85–112. https://doi.org/10.1016/j.ensm.2019.06.036.

Liu, T., Liu, Y., Wang, X., Kong, X., and Li, G. (2019). Cooling control of thermally-induced thermal runaway in 18,650 lithium ion battery with water mist. Energy Convers. Manage. *199*, 111969. https://doi.org/10.1016/j.enconman.2019.111969.

Liu, T., Tao, C., and Wang, X. (2020b). Cooling control effect of water mist on thermal runaway propagation in lithium ion battery modules. Appl. Energy *267*. https://doi.org/10.1016/j.apenergy.2020.115087.

Lu, T.-Y., Chiang, C.-C., Wu, S.-H., Chen, K.-C., Lin, S.-J., Wen, C.-Y., and Shu, C.-M. (2013). Thermal hazard evaluations of 18650 lithium-ion batteries by an adiabatic calorimeter. J. Therm. Anal. Calorim. *114*, 1083–1088. https://doi.org/10.1007/s10973-013-3137-9.

Maloney, T. (2014). Extinguishment of Lithium-Ion and Lithium-Metal Battery Fires (US Federal Aviation Administration).

Mao, B., Huang, P., Chen, H., Wang, Q., and Sun, J. (2020). Self-heating reaction and thermal runaway criticality of the lithium ion battery. Int. J. Heat Mass Transfer *149*, 119178. https://doi.org/10.1016/j.ijheatmasstransfer.2019.119178.

Meng, X., Yang, K., Zhang, M., Gao, F., Liu, Y., Duan, Q., and Wang, Q. (2020). Experimental study on combustion behavior and fire extinguishing of lithium iron phosphate battery. J. Energy Storage *30*, 101532. https://doi.org/10.1016/j.est.2020.101532.

Mohammed, A.H., Esmaeeli, R., Aliniagerdroudbari, H., Alhadri, M., Hashemi, S.R., Nadkarni, G., and Farhad, S. (2019). Dual-purpose cooling plate for thermal management of prismatic lithium-ion batteries during normal operation and thermal runaway. Appl. Therm. Eng. *160*, 114106. https://doi.org/10.1016/j.applthermaleng.2019.114106.

Ni, X., and Chow, W.K. (2011). Performance evaluation of water mist with bromofluoropropene in suppressing gasoline pool fires. Appl. Therm. Eng. *31*, 3864–3870.

https://doi.org/10.1016/j.applthermaleng.2011.07.034.

Payri, R., Gimeno, J., Martí-Aldaraví, P., and Carvallo, C. (2020). Parametrical study of the dispersion of an alternative fire suppression agent through a real-size extinguisher system nozzle under realistic aircraft cargo cabin conditions. Process Saf. Environ. Prot. *141*, 110–122. https://doi.org/10.1016/j.psep.2020.04.022.

Qin, P., Liao, M., Zhang, D., Liu, Y., Sun, J., and Wang, Q. (2019). Experimental and numerical study on a novel hybrid battery thermal management system integrated forced-air convection and phase change material. Energy Convers. Management *195*, 1371–1381. https://doi.org/10.1016/j.enconman.2019.05.084.

Ren, D., Feng, X., Lu, L., He, X., and Ouyang, M. (2019). Overcharge behaviors and failure mechanism of lithium-ion batteries under different test conditions. Appl. Energy *250*, 323–332. https://doi.org/10.1016/j.apenergy.2019.05.015.

Said, A.O., Lee, C., and Stoliarov, S.I. (2020). Experimental investigation of cascading failure in 18650 lithium ion cell arrays: impact of cathode chemistry. J. Power Sourc. *446*, 227347. https://doi.org/10.1016/j.jpowsour.2019.227347.

Somandepalli, V., Marr, K., and Horn, Q. (2014). Quantification of combustion hazards of thermal runaway failures in lithium-ion batteries. SAE Int. *3*, 98–104. https://doi.org/10.4271/2014-01-1857.

Tang, X., Wang, Y., Cui, J., Hu, X., Bi, S., and Wu, J. (2020). Thermal diffusivity measurement of trans-1-chloro-3,3,3-trifluoropropene (R1233zd(E)) and dodecafluoro-2-methylpentan-3-one (Novec1230) by the dynamic light scattering method. J. Chem. Eng. Data *65*, 4236–4241. https://doi.org/10.1021/acs.jced.0c00221.

Wang, H., Chen, X., Guo, J., Shen, J., Xie, S., and He, Y. (2019a). Fire Extinguishing Experiments on the Lithium Battery in Civil Aircraft Transport under a Variable-Pressure Environment (IEEE)), pp. 1–6.

Wang, Q., Li, K., Wang, Y., Chen, H., Duan, Q., and Sun, J. (2018). The efficiency of dodecafluoro-2-methylpentan-3-one on suppressing the lithium ion battery fire. J. Electrochem. Energy Convers. Storage *15*, 04100110. https://doi.org/10.1115/1.4039418.

Wang, Q., Shao, G., Duan, Q., Chen, M., Li, Y., Wu, K., Liu, B., Peng, P., and Sun, J. (2015). The efficiency of heptafluoropropane fire extinguishing agent on suppressing the lithium titanate battery fire. Fire Technol. *52*, 387–396. https://doi.org/10.1007/s10694-015-0531-9.

Wang, Z., Sun, F., and Liu, P. (2017). Electric Vehicle Battery Systems.

Wang, Z., and Wang, J. (2020). An experimental investigation of the degradation and combustion behaviors associated with lithium ion batteries after different aging treatments. J. Clean. Prod. *272*, 122708. https://doi.org/10.1016/j.jclepro.2020.122708.

Wang, Z., Yang, H., Li, Y., Wang, G., and Wang, J. (2019b). Thermal runaway and fire behaviors of large-scale lithium ion batteries with different heating methods. J. Hazard Mater. *379*, 120730. https://doi.org/10.1016/j.jhazmat.2019.06.007.

Weng, J., Yang, X., Ouyang, D., Chen, M., Zhang, G., and Wang, J. (2019). Comparative study on the transversal/lengthwise thermal failure propagation and heating position effect of lithium-ion batteries. Appl. Energy *255*, 113761. https://doi.org/10.1016/j.apenergy.2019.113761.

Xu, C., Zhang, F., Feng, X., Jiang, F., Ren, D., Lu, L., Yang, Y., Liu, G., Han, X., Friess, B., and Ouyang, M. (2021). Experimental study on thermal runaway propagation of lithium-ion battery modules with different parallel-series hybrid connections. J. Clean. Prod. *284*, 124749. https://doi.org/10.1016/j.jclepro.2020.124749.

Yiding, L., Wenwei, W., Cheng, L., Xiaoguang, Y., and Fenghao, Z. (2020). Multi-physics safety model based on structure damage for lithium-ion battery under mechanical abuse. J. Clean. Prod. *277*, 124094. https://doi.org/10.1016/j.jclepro.2020.124094.

Yu, M., Wan, S., Xu, Y., Zheng, K., and Liang, D. (2016). Suppressing methane explosion overpressure using a charged water mist containing a NaCl additive. J. Nat. Gas Sci. Eng. *29*, 21–29. https://doi.org/10.1016/j.jngse.2015.12.040.

Zhang, Y., Wang, H., Li, W., and Li, C. (2019). Quantitative identification of emissions from abused prismatic Ni-rich lithium-ion batteries. eTransportation *2*, 100031. https://doi.org/10.1016/j.etran.2019.100031.

Zhao, J., Fu, Y., Yin, Z., Xing, H., Lu, S., and Zhang, H. (2020a). Preparation of hydrophobic and oleophobic fine sodium bicarbonate by gel-sol-gel method and enhanced fire extinguishing performance. Mater. Des. *186*, 108331. https://doi.org/10.1016/j.matdes.2019.108331.

Zhao, J., Lu, S., Fu, Y., Shahid, M.U., and Zhang, H. (2020b). Application of ultra-fine dry chemicals modified by POTS/OBS for suppressing aviation kerosene pool fire. Fire Saf. J. *118*, 103148. https://doi.org/10.1016/j.firesaf.2020.103148.

Zhao, J., Yin, Z., Usman Shahid, M., Xing, H., Cheng, X., Fu, Y., and Lu, S. (2019). Superhydrophobic and oleophobic ultra-fine dry chemical agent with higher chemical activity and longer fire-protection. J. Hazard Mater. *380*, 120625. https://doi.org/10.1016/j.jhazmat.2019.05.018.

Zhong, G., Li, H., Wang, C., Xu, K., and Wang, Q. (2018). Experimental analysis of thermal runaway propagation risk within 18650 lithium-ion battery modules. J. Electrochem. Soc. *165*, A1925–A1934. https://doi.org/10.1149/2.0461809jes.

Zhu, J., Wierzbicki, T., and Li, W. (2018). A review of safety-focused mechanical modeling of commercial lithium-ion batteries. J. Power Sourc. *378*, 153–168. https://doi.org/10.1016/j.jpowsour.2017.12.034.

Zhu, J., Zhang, X., Sahraei, E., and Wierzbicki, T. (2016). Deformation and failure mechanisms of 18650 battery cells under axial compression. J. Power Sourc. *336*, 332–340. https://doi.org/10.1016/j.jpowsour.2016.10.064.

STAR★METHODS

KEY RESOURCES TABLE

REAGENT or RESOURCE	SOURCE	IDENTIFIER
Critical commercial assays		
Battery	Samsung	ICR18650-26JM
ABC ultra-fine powder	Shandong Guotai Technology Co, Ltd	FMY-GT
BC ultra-fine powder	Shandong Guotai Technology Co, Ltd	N/A
Perfluorohexanone	3M	Novec 1230
Software and algorithms		
Origin 2020	Originlab	http://www.OriginLab.com
BTS 7.6.0	Neware	https://www.neware.com.cn/software_support/

RESOURCE AVAILABILITY

Lead contact

Further information and requests should be directed to and will be fulfilled by the lead contact, Yangyang Fu (yyfu@ustc.edu.cn)

Materials availability

This study did not generate any new materials.

Data and code availability

We do not have any code and upon request we can provide the original data.

METHOD DETAILS

The pretreatment of 18650 batteries

The type of 18650 LIB was used in the experiments with the diameter of 18 mm, length of 65 mm. The total electric energy of the LIB was 2.6 Ah with the nominal voltage of 3.7 V. The plastic packaging was removed from all LIBs before testing and the resulting mass was 40.6 $\pm$ 0.1 g. The anode and cathode materials were based on intercalation graphite and lithiated metal oxide (Cobalt, Nickel, Manganese), respectively. To fully activate the LIB and show the maximum potential hazard of the LIB fires, the LIB used needed to undergo charge and discharge circles. First, the LIB was charged to 4.2 V at a constant current of 0.5 C (1200 mA), and then charged constantly under the voltage of 4.2V until the current reached 0.01 C (24 mA) under 25 $\pm$ 2°C. After that, the cell was discharged to 2.75V at a constant current of 1 C (2.40 A). Repeated this process 5 times and then charged to the specified SOC.

The choice of fire extinguishing agents

Four types of fire extinguishing agents were used here (i.e. water spray, ABC and BC ultra-fine dry powder, Novec 1230). Water was for domestic. ABC and BC ultra-fine dry powders were purchased from Shandong Guotai Technology Co, Ltd. The particle size distribution curves were shown in Figure S3. The particle size distribution was measured by a laser particle size analyzer (Type: SALD-2300, Shimadzu Corporation of Japan). The D_{90} particle diameters of ABC and BC powders were 1.1 μm and 2.3 μm, respectively. The main components of ABC and BC ultra-fine powders could be seen in Table S2. Novec 1230 was purchased from Sinochem Lantian Co, Ltd. The relative parameters of Novec 1230 were shown in Table S3.

The TR pretest layout of single LIB and LIB arrays

Before fire extinguishing experiments, the TR behaviors of single LIB and propagation characteristics of LIB arrays were tested. The five typical SOCs (i.e., 0%, 30%, 50%, 70% and 100%) were selected. The heater and

four LIBs were placed in a row. Two thermocouples are arranged for each LIB to measure the side and bottom temperatures, as shown in Figure S4.

During experiments, LIBs vibrated when TR occurred, which caused thermocouples failed. Thus, the temperature data were not convincing. In present work, iron wires or Teflon tapes were used for fixing the thermocouples (Liu et al., 2019; Weng et al., 2019). However, it caused gaps between LIBs and affected the TR propagation, leading errors to the measured data. To avoid errors, nickel sheets were welded on the LIB surfaces and thermocouples were inserted into gaps. It was found that the way could ensure the detected temperature data repeatable and accurate. An adjustable clamp made of aluminum alloy was used to fix the heater and LIBs in a row. To avoid heat conduction between clamp and LIBs, aerogel felts were filled into interspaces as the insulation to ensure the heat conduction between LIBs. Each test was repeated at least twice.

Experimental setup of fire extinguishing on the TR inhibition of LIB arrays

A schematic diagram of the experimental set was shown in Figure S5. The experiments were done in a LIB experimental box, with an internal volume of 216 L. The overall size of the LIB box was 900 mm×870 mm×1010 mm. The fire extinguishing agent release system included a gas cylinder, a container, valves, connecting hose and a nozzle. Before tests, open valve 1 and fill the tank to 1.2 Mpa. Valve 2 was a 24 V DC powered solenoid valve with a time relay. To ensure the fire extinguishing agents were not spraying out with in specified time, the spraying duration was set as 20 s. LIB arrays including four LIBs were triggered TR by a 100 W heater with the same size as 18650 LIB. The LIBs would be triggered one by one. The diameter of the nozzle was 2 mm with the spraying distance of 35 mm.

The data acquisition system was composed of video acquisition, temperature data acquisition and gas analyzer. Thermocouples with a diameter of 1 mm were used to measure the upper and lower surfaces of LIB, respectively. The electrical signal was processed by the Agilent 34970A and then converted into temperature signal. The temperature data was finally recorded to the computer. CO was one of the main gas produced during the TR process of LIBs (Chen et al., 2020; Li et al., 2019b). Thus, the gas analyzer was used to monitor CO concentration of the box. Each test was repeated at least twice.